

# Fully self-consistent calculations of nuclear Schiff moments

Shufang Ban,<sup>1,2</sup> Jacek Dobaczewski,<sup>3,4</sup> Jonathan Engel,<sup>1</sup> and A. Shukla<sup>1,5</sup>

<sup>1</sup>*Dept. of Physics and Astronomy, University of North Carolina, Chapel Hill, NC, 27516-3255, USA*

<sup>2</sup>*Nuclear Theory Center and Department of Physics, Indiana University, 701 E. Third St., Bloomington, IN, 47405, USA*

<sup>3</sup>*Institute of Theoretical Physics, Warsaw University ul. Hoza 69, PL-00681 Warsaw, Poland*

<sup>4</sup>*Department of Physics, P.O. Box 35 (YFL), FI-40014 University of Jyväskylä, Finland*

<sup>5</sup>*Rajiv Gandhi Institute of Petroleum Technology, Ratapur Chowk, Raebareli -229316, U.P., India*

We calculate the Schiff moments of the nuclei  $^{199}\text{Hg}$  and  $^{211}\text{Ra}$  in completely self-consistent odd-nucleus mean-field theory by modifying the Hartree-Fock-Bogoliubov code HFODD. We allow for arbitrary shape deformation, and include the effects of nucleon dipole moments alongside those of a CP-violating pion-exchange nucleon-nucleon interaction. The results for  $^{199}\text{Hg}$  differ significantly from those of previous calculations when the CP-violating interaction is of isovector character.

PACS numbers: 11.30.Er, 21.60.Jz

## I. INTRODUCTION

There are compelling reasons to believe in a source of measurable CP violation from outside the Standard Model of particle physics. Supersymmetry and other theories that lessen the hierarchy problem<sup>1</sup> typically introduce many new fields with CP-violating phases into Lagrangians. If unsuppressed, such phases should be observable, now or in the foreseeable future. And they are needed if the imbalance between matter and antimatter in the universe is the result of a CP asymmetry; in the Standard Model CP violation is too weak to be responsible [2].

As long as the CPT theorem holds, one can search for time-reversal (T) violation in lieu of CP violation. One of the best ways to observe T violation from beyond the Standard Model is by measuring nonzero static electric dipole moments (EDMs) in systems with non-degenerate ground states. Standard-Model CP violation is suppressed in flavor-conserving processes, so an observed EDM anywhere near current limits would imply new physics. Experimental groups have been steadily lowering the upper limits on EDMs to the point that one might reasonably expect an observation in the near future. (Much of supersymmetry parameter space has already been covered.) For now, the nonobservation of an EDM in the diamagnetic atom  $^{199}\text{Hg}$  places tight upper limits on CP violation, and measurements in other diamagnetic systems —  $^{129}\text{Xe}$ ,  $^{223,225}\text{Ra}$ , and  $^{223}\text{Rn}$  — may soon do even better.

Whether these experiments eventually see a nonzero EDM or just continue to set limits, their interpretation requires us to understand the dependence of atomic EDMs on the strength of CP violation at the fundamental level. Doing so involves calculations at several scales. QCD determines the dependence on fundamental physics

of the neutron EDM and related quantities such as effective P- and T-violating meson-nucleon coupling constants. Nuclear physics then translates these quantities into P- and T-violating nuclear moments, which in turn contribute to atomic EDMs.

The role of nuclear physics in this chain is more subtle than it appears at first glance because the atomic electrons screen nuclear EDMs [3]. As a result, the nuclear quantity that plays the largest role in inducing atomic EDMs is not the nuclear dipole moment, but rather the “Schiff moment”,

$$S \equiv \langle 0 | S_z | 0 \rangle_{M=J} , \quad (1)$$

that is, the ground state expectation value (in the substate that is fully polarized along the  $z$  axis) of the  $z$ -component of the one-body “Schiff operator.” This vector operator is given approximately by

$$\mathbf{S} = \mathbf{S}^{\text{ch}} + \mathbf{S}^{\text{nucleon}} , \quad (2)$$

where

$$\mathbf{S}^{\text{ch}} = \frac{e}{10} \sum_{p=1}^Z \left( r_p^2 - \frac{5}{3} \langle r^2 \rangle_{\text{ch}} \right) \mathbf{r}_p . \quad (3)$$

$$\begin{aligned} \mathbf{S}^{\text{nucleon}} = & \frac{1}{6} \sum_{j=1}^A \mathbf{d}_j (r_j^2 - \langle r^2 \rangle_{\text{ch}}) \\ & + \frac{1}{5} \sum_{j=1}^A \left( \mathbf{r}_j (\mathbf{r}_j \cdot \mathbf{d}_j) - \frac{r_j^2}{3} \mathbf{d}_j \right) + \dots \end{aligned} \quad (4)$$

Here  $e$  is the charge of the proton,  $\langle r^2 \rangle_{\text{ch}}$  is the mean squared radius of the nuclear charge distribution,  $\mathbf{d}_j$  is the EDM of nucleon  $j$ , and the omitted terms in Eq. (4) are smaller than those included by about the square of the ratio of the proton radius to the nuclear radius. The sum in Eq. (4) is over all nucleons, while that in Eq. (3) is restricted to protons.

The two terms in Eq. (2) reflect the two ways in which a nucleus can acquire Schiff moments. A P-

<sup>1</sup> See, e.g., Ref. [1] for a short but clear statement of the problem.

and T-violating nucleon-nucleon interaction generates a corresponding charge distribution and a contribution to  $S$  from the operator  $\mathbf{S}^{\text{ch}}$  in Eq. (3), while nucleon EDMs generate a contribution from  $\mathbf{S}^{\text{nucleon}}$  in Eq. (4). Both contributions can be induced by effective P- and T-violating pion-nucleon coupling constants: a pion-exchange graph with one such coupling generates the effective nucleon-nucleon interaction and a pion loop graph with one generates nucleon EDMs. The two-body interaction is

$$V_{PT} = \frac{g}{8\pi m_N} \sum_{i < j} \left\{ \left[ \bar{g}_0 (\boldsymbol{\tau}_i \cdot \boldsymbol{\tau}_j) - \frac{\bar{g}_1}{2} (\tau_i^z + \tau_j^z) + \bar{g}_2 (3\tau_i^z \tau_j^z - \boldsymbol{\tau}_i \cdot \boldsymbol{\tau}_j) \right] (\boldsymbol{\sigma}_i - \boldsymbol{\sigma}_j) - \frac{\bar{g}_1}{2} (\tau_i^z - \tau_j^z) (\boldsymbol{\sigma}_i + \boldsymbol{\sigma}_j) \right\} \cdot \boldsymbol{\nabla}_i \frac{\exp(-m_\pi |\mathbf{r}_i - \mathbf{r}_j|)}{|\mathbf{r}_i - \mathbf{r}_j|}, \quad (5)$$

and the nucleon EDM operator (for nucleon  $j$ ), in the leading chiral approximation<sup>2</sup> is

$$\mathbf{d}_j = \frac{eg}{4\pi^2 m_N} \ln \frac{m_N}{m_\pi} (\bar{g}_0 - \bar{g}_2) \boldsymbol{\sigma}_j \tau_j^z, \quad (6)$$

In these two equations  $\hbar = c = 1$ ,  $m_\pi$  is the mass of the pion,  $m_N$  is that of the nucleon,  $\tau^z$  gives +1 when acting on a neutron,  $g \equiv 13.5$  is the strong  $\pi$ NN coupling constant, and the  $\bar{g}_i$  are dimensionless isoscalar ( $i = 0$ ), isovector ( $i = 1$ ), and isotensor ( $i = 2$ ) P- and T-violating  $\pi$ NN coupling constants. These last quantities depend on the unknown fundamental source of CP violation, and so are primitive in our treatment. A QCD calculation can in principle relate them to quantities in extra-Standard-Model theories.

Since  $V_{PT}$  is extremely weak and the nucleon EDM in Eq. (6) is extremely small, the Schiff moment, to very high accuracy, is linear in the  $\pi$ NN couplings  $\bar{g}_i$ . We write it as

$$S = (a_0 + b) g \bar{g}_0 + a_1 g \bar{g}_1 + (a_2 - b) g \bar{g}_2. \quad (7)$$

The  $a_i$  specify the dependence of  $S$  on the P- and T-violating interaction  $V_{PT}$ , and  $b$  specifies its dependence on the nucleon dipole moments  $\mathbf{d}_j$ . All relevant nuclear structure information is encoded in these coefficients.

The  $a_i$  have been calculated before, with varying degrees of sophistication, in nuclei used in or considered for experiments. Except in a few nuclei with strong octupole deformation, all prior has proceeded in two steps: some kind of mean-field calculation in which the polarizing effects of the last (valence) nucleon were neglected,

followed by an explicit treatment of the correlations induced by the interaction of the valence nucleon with the rest. Ref. [5], the first such calculation, used a phenomenological Wood-Saxon potential as the mean field and allowed the valence-core interaction to excite only non-collective one-particle one-hole configurations. Refs. [6] and [7] obtained the mean field through an approximate Hartree-Fock calculation and used a simple residual strong interaction and linear-response theory (that is, the random phase approximation (RPA)) to include collective corrections to the simple excitations considered in Ref. [5]. Finally, Ref. [8] carried out a self-consistent Skyrme-interaction-based calculation to obtain the mean field, and followed that with a diagrammatic treatment (with the same Skyrme interaction) of most but not all of the quasiparticle-RPA (QRPA) response generated by the valence-core interaction.

In the work reported here, we modify the Hartree-Fock-Bogoliubov code HFODD [9] to carry out completely self-consistent mean-field calculations directly in the nuclei of interest. That is, we

1. treat  $V_{PT}$  on the same footing as the strong interaction,
2. treat all the nucleons, including the last, on the same footing in mean-field theory.

These steps make our treatment essentially equivalent to a fully self-consistent treatment of the even nucleus followed by the self-consistent inclusion of all linear-response collectivity induced by the valence-core interaction. Thus, unlike the work of Refs. [6, 7] our calculation is completely self consistent, and unlike the work of Ref. [8] it includes all core-polarization effects, in a unified way to boot. In addition, our mean-field can (and often will) be deformed. All prior calculations in systems without octupole deformation assumed spherical ground states. In nuclei such as <sup>199</sup>Hg the quadrupole deformation may well be large enough to affect Schiff moments; the successful Möller-Nix phenomenology [10] predicts deformation parameters  $\beta_2 = -0.122$  and  $\beta_4 = -0.032$ , values that are hardly negligible. Finally, we project our states onto those with well-defined angular momentum (after variation), going beyond the usual rigid-rotor approximation. This step is essential in nuclei that are only weakly deformed.

## II. METHOD AND TESTS

We begin with a more precise statement of the relation between the perturbative treatment of interactions within linear-response theory, that is, the RPA or QRPA, and a non-perturbative treatment in mean-field theory. Consider, for example, an even-even nucleus with  $Z + N = A$  nucleons, neglecting pairing temporarily to simplify the situation. It is not hard to show [11, 12] that the one-body density matrix obtained from a Hartree-Fock (HF) calculation in the neighboring odd nucleus

<sup>2</sup> Nucleons can get EDMs in other ways, e.g. from quark EDMs [4], but we assume here for simplicity that the  $\bar{g}_i$  are the only relevant low-energy CP-violating parameters. The dependence of nuclear Schiff moments on the nucleon EDMs, no matter what their source, can be extracted from our analysis by dividing out the  $\bar{g}$ -dependent prefactor in Eq. (6).

with one more neutron is related to that obtained from a corresponding (much easier) calculation in the even nucleus by:

$$\rho_{a,b}^{A+1} = \rho_{a,b}^A + \rho_{a,b}^v + \sum_{c,d} R_{ab,cd}^A h_{cd}^v + \dots \quad (8)$$

where  $\rho^{A+1}$  and  $\rho^A$  are density matrices (isoscalar or isovector) for the odd and even nuclei,  $\rho^v$  is the density matrix associated with the valence neutron in the first empty orbit produced by the even-nucleus mean field,  $h^v$  is the additional mean-field Hamiltonian created by that valence nucleon,  $R^A$  is the zero-frequency RPA response function for the even-even core, and the neglected terms are higher order in  $h^v$ . Eq. (8) generalizes predictably when pairing is included via Hartree-Fock-Bogoliubov (HFB) theory and the QRPA. When the interaction  $V_{PT}$  is included, it affects Schiff moments only through the last term.

We can now more precisely characterize previous calculations, which were based on approximate representations of the right-hand side of Eq. (8). Refs. [6, 7] used a simple Landau-Migdal strong interaction and approximate self consistency in determining the densities and RPA response function  $R^A$ , and treated  $V_{PT}$  without further approximation. Ref. [8] used full-fledged Skyrme interactions and retained self consistency everywhere, but obtained the response function  $R_A$  by first neglecting  $V_{PT}$ , then adding first-order corrections through a series of diagrams, some of which were omitted. Both calculations imposed spherical symmetry everywhere. Here we calculate the left-hand side of Eq. (8) directly in mean field theory, without the intermediary of response functions and with no approximations or imposed symmetries. Of course, the Skyrme interactions we use are not perfect, but they are the current state of the art.

Mean-field calculations in odd nuclei are notoriously tricky [13]. Because the valence nucleon can polarize the rest, odd systems are more likely than their even-even neighbors to have complicated triaxial shapes;  $^{129}\text{Xe}$ , which has a tight limit on its atomic EDM, is an example. Unless one projects triaxial intrinsic states onto states with good angular momentum before the mean-field variation, it is difficult to ensure that the component with the correct angular momentum is a significant part of the wave function. Moreover, triaxial systems are often soft, meaning that the wave function corresponding to the absolute minimum energy may not more significantly represent the nuclear state than other wave functions with only slightly higher energies. We therefore will restrict ourselves to axially symmetric systems in which the spin aligns along the symmetry axis; in such states we can ensure a significant component with a given  $J$  by selecting states for which the intrinsic angular momentum z-projection  $K$  is equal to  $J$ . We sometimes pay the price that the desirable configurations are not the lowest ones and that are solutions are marginally unstable; we discuss those difficulties below.

To implement our procedure, we employ a modified version of the state-of-the-art code HFODD (see Ref. [9] and references therein), which uses a symmetry-unrestricted three-dimensional harmonic-oscillator (HO) basis to carry out Skyrme HF or HFB calculations. Our modification is to add  $V_{PT}$  to the Skyrme interaction, allowing the calculation of Schiff moments. An initial step, reported in Ref. [14], was to represent  $V_{PT}$  as a sum of Gaussians in order to ease calculation in the HO basis, and evaluate its expectation value at the end of the calculation in octupole-deformed nuclei. Here we extend that scheme and incorporate it into the self-consistent loop; the code evaluates the expectation value of  $V_{PT}$  and the corresponding mean fields, which are the new ingredient, at every iteration. (We have actually coded the mean fields only in the normal particle-hole mean channel; we deal with the pairing field through a trick discussed below.) It then adds the P- and T-violating mean fields to those coming from the Skyrme interaction, so that all forces are treated in the same way. The resulting P- and T-violating polarization produces a nonzero expectation value for the Schiff operator  $S_z^{\text{ch}}$  in Eq. (3). To calculate the expectation value of  $S_z^{\text{nucleon}}$ , we simply use the HF or HFB wave functions obtained without the addition of  $V_{PT}$ .

To check the results, we also incorporate the direct part of  $V_{PT}$  in a completely different way. The direct P- and T-violating mean field can be written<sup>3</sup> as

$$v_{PT}^d = \frac{g}{8\pi m_N} \int d\mathbf{r}' \frac{e^{-m_\pi|\mathbf{r}-\mathbf{r}'|}}{|\mathbf{r}-\mathbf{r}'|} \times \left\{ [\bar{g}_1 - (\bar{g}_0 + 2\bar{g}_2)\tau_z] \nabla \cdot \mathbf{s}_1(\mathbf{r}') + \sigma\tau_z \cdot \{(\bar{g}_0 + 2\bar{g}_2)\nabla\rho_1(\mathbf{r}') - \bar{g}_1\nabla\rho_0(\mathbf{r}')\} \right\}, \quad (9)$$

where  $\mathbf{s}_1$  is the isovector spin density (see the appendix of Ref. [16], where the density is called  $\mathbf{s}_{10}$ , for the exact definition), and  $\rho_0$ ,  $\rho_1$  are the usual isoscalar and isovector number densities. This representation as the folding of a Yukawa function with a source density is similar to the representation of the Coulomb potential as the folding of the function  $1/|\mathbf{r}-\mathbf{r}'|$  with the charge density. We therefore adapt the existing Green-function-based routine for calculating the direct Coulomb potential in HFODD to the evaluation of the direct P- and T-violating mean field  $v_{PT}^d$ .

Finally, to further check the self-consistent solution, we note that before projection in an axially symmetric nucleus, one should obtain the same Schiff moment to leading order in an arbitrary constant  $\lambda$  by

- a) Solving self-consistent field equations with  $H \equiv H_{\text{Skyrme}} + \lambda V_{PT}$ , and then evaluating the expectation value of  $S_z^{\text{ch}}/\lambda$ ,

<sup>3</sup> The term containing  $\mathbf{s}_1$  was omitted in Ref. [15]

- b) Solving the mean-field equations with  $H \equiv H_{\text{Skyrme}} + \lambda S_z^{\text{ch}}$  and then evaluating the expectation value of  $V_{PT}/\lambda$ .
- c) Solving the mean-field equations with  $H \equiv H_{\text{Skyrme}}$  and then evaluating

$$\sum_i \frac{\langle 0 | S_z^{\text{ch}} | i \rangle_{\text{RPA}} \langle i | V_{PT} | 0 \rangle_{\text{RPA}}}{(E_0 - E_i)} + c.c., \quad (10)$$

where the subscripts on the kets mean that the transition matrix elements are evaluated in RPA (or QRPA). Procedure a) above defines the problem we're trying to solve. Procedure b) serves as a check and, moreover, is our primary procedure in nuclei with pairing. The reason, as mentioned above, is that although we can evaluate the expectation value of  $V_{PT}$  (including the pairing parts), we cannot evaluate the corresponding pairing field, so that we cannot include all the effects of pairing in procedure a). Finally, regarding the RPA or QRPA: although we cannot do an RPA or QRPA calculation in a deformed or odd-A nucleus, we can use procedure c) as a test in a spherical nucleus. A full odd-A QRPA evaluation, even there, would involve adding all the complicated diagrams in Ref. [8], so we make our test in the approximation that last nucleon feels the strong mean-field from the other nucleons but acts on them in turn only weakly (through  $V_{PT}$ ). This makes it sufficient to apply the QRPA to the even-even core.

To implement this ‘‘weak-valence-field’’ approximation, in a closed-shell+1 nucleus such as  $^{57}\text{Ni}$ , we first calculate the self-consistent ground-state in the even-even neighbor  $^{56}\text{Ni}$  without including  $V_{PT}$  in the Hamiltonian, and then allow the valence neutron to occupy the first empty neutron orbit. We then calculate the P- and T-violating mean field that that neutron produces (restricting ourselves for simplicity to the dominant direct part) by evaluating its contribution to  $v_{PT}^d$  in Eq. (9). We then use this mean field as an external P- and T-violating source for the  $^{56}\text{Ni}$  core. The Schiff moment of  $^{57}\text{Ni}$  in the weak-valence-field approximation is then the moment of the  $A = 56$  core induced by the external source.

We can implement the procedure in mean-field theory by adding the external source  $v_{PT}^d$  or  $S_z^{\text{ch}}$  for  $^{56}\text{Ni}$  to  $H_{\text{Skyrme}}$  as in procedure a) or b) above, or in the RPA by substituting  $v_{PT}^d$  for  $V_{PT}$  in procedure c). The first two routes are straightforward and give identical results but the spherical RPA requires a decomposition of  $v_{PT}^d$  into spherical multipoles. To make that simpler, we use the zero-range (infinite pion-mass) approximation, which reduces the Yukawa function in Eq. (9) to a delta function, when carrying out any of the three procedures a), b), and c). Even so, we can always expect slight differences between the results of procedure c) and the others because of slight differences in the single-particle spaces underlying the mean-field and RPA calculations. In the former, we include single-particle HO basis states with up to 22  $\hbar\omega$  of excitation energy. In the latter, which we

TABLE I: HFODD and RPA results with the Skyrme interaction SkM\* for the coefficients  $a_i$ , in  $e\text{fm}^3$ , in the weak-valence-field approximation (see text) in  $^{57}\text{Ni}$  and  $^{209}\text{Pb}$ . We have omitted exchange terms in  $V_{PT}$  and taken the zero-range limit of the interaction. In this approximation  $a_2 = 2a_0$ .

		$a_0$	$a_1$
$^{57}\text{Ni}$	HFODD	-0.0222	-0.0536
	RPA	-0.0226	-0.0529
$^{209}\text{Pb}$	HFODD	-0.0466	-0.1059
	RPA	-0.0507	-0.1048

carry out with the spherical HFB code HFBRAD [17] and the QRPA code QRPA sph [18], we include single-particle spherical-box states with energies up to 100 MeV. Despite the single-particle differences, the results of the procedures a) and c), displayed in Tab. I for the Skyrme interaction SkM\* [19], are extremely close.

The table also compares the results of procedures<sup>4</sup> b) and c) for  $^{209}\text{Pb}$ , again with SkM\*. In this heavy nucleus we can include orbits with up to only 12  $\hbar\omega$  in HFODD, and while the mean-field and RPA results for  $a_1$  agree very well, those for  $a_0$  differ by about 10%. This small discrepancy is almost certainly due to the limited HFODD model space. Overall, the level of agreement, particularly in Ni where we are able to do the best job, convinces us that both kinds of calculations are essentially correct.

The weak-valence-field approximation is equivalent to including only ‘‘diagram A’’ from Ref. [8] in the RPA-based diagram sum that yields the Schiff moment. We should note that our results for  $^{209}\text{Pb}$  are significantly different from those for diagram A in the same nucleus given in the Ph.D. dissertation on which Ref. [8] was based. We discuss possible reasons for the discrepancy, which also exists in  $^{199}\text{Hg}$ , towards the end of this paper. For now, we simply note that accurate RPA calculations require a more careful job than one might think. Figure 1 shows the summed contributions of excited RPA states in Eq. (10) to the  $a_i$ . The coefficient  $a_1$  is nearly constant after 50 MeV, but  $a_0$  continues to decrease even at 80 MeV. Most RPA calculations do not go that high in excitation energy, or if they do they make approximations that can alter results significantly.

### III. RESULTS

We turn now to the full calculations in nuclei of interest for experiment. We apply our mean-field techniques to  $^{211}\text{Ra}$  and  $^{199}\text{Hg}$ . The first is one of the Radon isotopes to be explored at TRIUMF [20] and the second is

<sup>4</sup> In this nucleus, an accurate mean-field result requires dealing with the center-of-mass shift that results from the fixed external source  $v_{PT}^d$ ; the task is easier in procedure b) than in a).

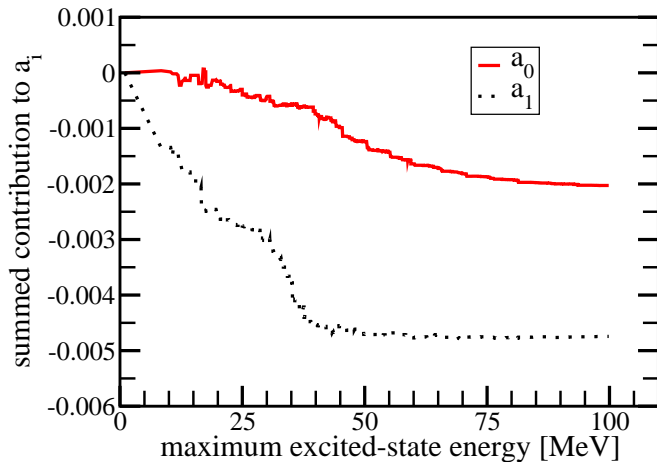


FIG. 1: (Color online.) The summed RPA contributions to the  $a_i$  in  $^{57}\text{Ni}$ , in the “weak-valence-interaction” approximation, as a function of excited-state energy.

the nucleus with the best current limit on its Schiff moment. We use several Skyrme interactions: SLy4 [21], SkM\* [19], SV [22], and SIII [22]. The last of these may not be as trustworthy as the others; Ref. [8] showed that the interaction was less able to reproduce a related observable, the distribution of isoscalar  $E1$  strength in even nuclei. In previous work we have employed SkO’ [23]. We were not able to find an axially symmetric ground state in  $^{199}\text{Hg}$  with that interaction, however, and so do not use it here.

The nucleus  $^{211}\text{Ra}$  is spherical, so the calculation there is relatively straightforward. We start with an HFB calculation with  $H_{\text{Skyrme}}$  only. Since the ground state has  $J^\pi = \frac{1}{2}^-$ , we must block the lowest  $\Omega^\pi = \frac{1}{2}^-$  level, which because of the spherical shape is essentially the  $3p_{1/2}$  orbit ( $\Omega$  is the  $z$ -projection of the angular momentum in the intrinsic frame). We then obtain the coefficient  $b$  by simply evaluating the expectation value of  $S_z^{\text{nucleon}}/\bar{g}_0$ , with an arbitrary value chosen for  $\bar{g}_0$  and  $\bar{g}_2$  set to zero. To obtain the coefficients  $a_i$ , we follow procedure a) above, successively setting each of the  $\bar{g}_i$  to one. The results for several Skyrme interactions appear in Table II.

The three Skyrme interactions we use give similar results, though the value of  $a_1$  produced by SIII is noticeably suppressed. The coefficient  $b$  is apparently less sensitive and usually somewhat smaller than the  $a_i$ . It is not small enough, however, to be neglected, as it has been in all prior work.

In  $^{199}\text{Hg}$  the calculation is harder because the nucleus

TABLE II: Results for coefficients  $a_i$  and  $b$ , in  $e \text{ fm}^3$ , in  $^{211}\text{Rn}$ .

	$a_0$	$a_1$	$a_2$	$b$
SLy4	0.042	-0.018	0.071	0.016
SkM*	0.042	-0.028	0.078	0.015
SIII	0.034	-0.0004	0.064	0.015

TABLE III: Results for coefficients  $a_i$  (in  $e \text{ fm}^3$ ) in  $^{199}\text{Hg}$ , with the Skyrme interaction SLy4, in various approximations. The solution is axially symmetric with  $\beta = -0.13$  and an excitation energy for the  $\Omega^\pi = \frac{1}{2}^-$  state of 0.97 MeV

	$a_0$	$a_1$	$a_2$
One HF iteration with $V_{PT}$	0.045	0.049	0.090
Full HF, no projection	0.039	-0.019	0.066
Full HF, projected	0.013	-0.006	0.022

may not be spherical, and is almost certainly soft. The energy as a function of deformation is probably very flat, and the energies of several mean-field minima may not be very different. For this reason, we do several calculations, some at deformed minima and some at spherical minima. Another issue is that HFODD cannot carry out angular-momentum projection if pairing is included. We can estimate the effects of projection, or turn pairing off and carry it out explicitly. We follow both courses here and compare the results. We sometimes encounter the further problem that the state with the correct ground-state quantum numbers ( $\Omega^\pi = \frac{1}{2}^-$ ) is not the lowest state in our calculation. In a soft nucleus, such an occurrence is not totally surprising.

Finally, the inclusion of  $V_{PT}$  causes some problems that are not present without it. Although  $V_{PT}$  is very weak, the iterative HF energy sometimes eventually diverges, probably because our axially symmetric excited-state solution is very slightly unstable against some kinds of asymmetric deformation. In such cases, however, the solution converges for awhile, coming quite close to self consistency, before the weak instability leads it in a different direction. We can therefore extract an axially-symmetric result from the relatively early iterations, during which the solution apparently converges. Although we don’t have a truly self-consistent solution here, we do obtain a kind of “most nearly self-consistent axially-symmetric” solution, which is the best we can do without the more difficult and possibly less meaningful task of considering triaxial shapes for soft systems.

Table III displays the results for the interaction SLy4 in successively better approximations. The first line shows the results after including  $V_{PT}$  for one Hartree-Fock iteration (starting from the converged solution with  $V_{PT}$  omitted). In this limit,  $V_{PT}$  can excite the core, but the excited nucleons do not further interact before contributing to the Schiff moment; that is, no core collectivity is included. A comparison of the first two lines shows, in agreement with Refs. [6–8], that collectivity has a large effect on the  $a$ ’s. But in contrast to those investigations, we find that collectivity has a large enough effect on  $a_1$  to change its sign. This change in sign appears in many of our other Hg calculations as well, even for spherical minima. Its appearance there is surprising because the diagrammatic calculation of Ref. [8] used the same Skyrme interactions and essentially the same spherical-

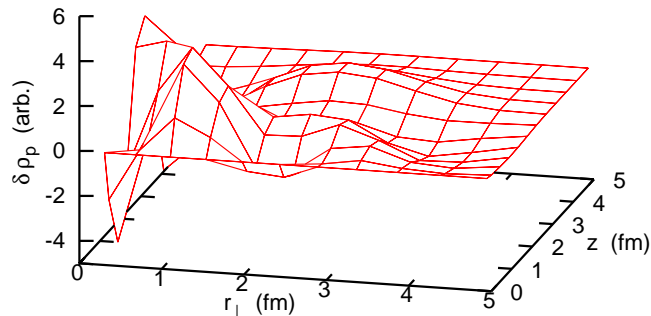


FIG. 2: (Color online.) The change in proton density induced by the  $\bar{g}_1$  term in  $V_{PT}$ , as a function of  $r_\perp \equiv \sqrt{x^2 + y^2}$  and  $z$ . The units are arbitrary because of the arbitrariness in the constant  $\bar{g}_1$ . Only 1/4 of the nuclear profile is shown; the density change is symmetric in  $r_\perp$  and antisymmetric in  $z$ . The densities were actually evaluated at  $13^2$  Gaussian integration points, a fact that explains the spikiness of the plot.

HFB starting point<sup>5</sup>, and included much of the same collective physics. We have already remarked, though, that where we can check the QRPA results (in  $^{209}\text{Pb}$ ) we do not agree with them.

Another surprising result is that projection reduces the coefficients by a factor that is very close to three, the same factor as in the rigid-rotor model. The reduction factor is nearly three with other Skyrme interactions as well. The relatively small deformation of  $^{199}\text{Hg}$  led us to expect a milder reduction.

What is unsurprising is that the  $a_i$  are delicate and very hard to predict ahead of time. Figure 2 shows the change in proton density  $\delta\rho_p$  caused by the inclusion alongside SLy4 of the  $\bar{g}_1$  term in  $V_{PT}$  (that is, the other  $\bar{g}$ 's are set to zero). The integral of this density difference over  $z$  and  $r_\perp \equiv \sqrt{x^2 + y^2}$ , weighted by  $(r^2 - 5/3 \langle r^2 \rangle_{\text{ch}})z$ , is what gives the intrinsic Schiff moment (before projection). The oscillations are actually even wilder than the figure shows; a deep trough is hidden behind large peak at small  $r_\perp$ . These oscillations make it hard to supply an explanation for the sign and magnitude of  $a_1$ .

We turn finally to the full results obtained by using the HO basis of up to 12  $\hbar\omega$  of excitation energy, displayed in Tab. IV. The top three lines give the results of deformed HF calculations (the calculation with SKM\* does not give a convergent axially-symmetric result). All the interactions under-bind the nucleus; the measured binding energy is 1573.19 MeV. With the interactions SLy4 and SV, the ground state, as discussed above, does not have the correct quantum numbers, and we are forced to use an excited particle-hole configuration that does. As also mentioned, the energy eventually begins to diverge from our solution, presumably because of a very weak

triaxial instability. By contrast, SIII gives the correct ground state, and no long-term divergence. After projection, all three calculations produce similar coefficients  $a_0$  and  $a_2$ , but  $a_1$  varies significantly, even in sign. We are unable to project the one-body densities that yield the  $b$  coefficient, so we take the reduction from the unprojected value to be the same as that of the  $a_i$ 's.

The middle two lines of Tab. IV show the results of HFB calculations, in which pairing is included. The SLy4 solution is deformed, and as mentioned above, we cannot project HFB states; we therefore use the rigid rotor limit to obtain the projected results in line 4. SKM\* has a spherical minimum when pairing is included, so no projection is necessary. The results of that calculation are similar to the unprojected results from deformed solutions. We conclude that the presence of deformation, at least in our approach, significantly decreases calculated Schiff moments.

We should note that we do not include the  $\mathcal{O}(\alpha^2)$  corrections to the Schiff moment (generating the “local dipole moment” [24]). Work in simple models suggests that these corrections to the  $a_i$  are on the order of 25%, though they could be a larger fraction if the lowest-order  $a_i$  are suppressed.

Our  $^{199}\text{Hg}$  results have some significant differences from those obtained previously. Those of the two most comprehensive calculations appear at the bottom of Tab. IV, with the average of several calculations presented for Ref. [8]. Our values of  $a_0$  and  $a_2$  are in reasonable agreement with those of Ref. [8], but, as already mentioned, those for  $a_1$  are smaller in magnitude and sometimes have the opposite sign. Deformation, of course, is one cause, but, as noted above, there is disagreement even with our spherical calculations. One source of difference may be our treatment of core polarization, which is more complete and self-consistent than that of the earlier papers; the use of a canonical basis state for the last neutron in Ref. [8] may be another. Finally, the disagreement

TABLE IV: Results for coefficients  $a_i$  and  $b$ , in  $e\text{fm}^3$ , in  $^{199}\text{Hg}$ . The third column gives ground-state energy in MeV, the fourth the deformation, and the fifth the excitation energy (also in MeV) of the lowest configuration with the same value of  $\Omega^\pi$  as the experimental ground state. The first three lines are in the HF approximation, while the next two are in the HFB approximation. The last two lines report results of previous work, with the numbers for Ref. [8] representing the average over several interactions.

	$E_{\text{gs}}$	$\beta$	$E_{\text{exc.}}$	$a_0$	$a_1$	$a_2$	$b$
SLy4	-1561.42	-0.13	0.97	0.013	-0.006	0.022	0.003
SIII	-1562.63	-0.11	0	0.012	0.005	0.016	0.004
SV	-1556.43	-0.11	0.68	0.009	-0.0001	0.016	0.002
SLy4	-1560.21	-0.10	0.83	0.013	-0.006	0.024	0.007
SkM*	-1564.03	0	0.82	0.041	-0.027	0.069	0.013
Ref. [6]	—	—	—	0.0004	0.055	0.009	—
Ref. [8]	—	—	—	0.007	0.071	0.018	—

<sup>5</sup> One difference is that the last neutron was in a canonical-basis quasiparticle state in that work.

between our QRPA tests discussed above and those in the framework of Ref. [8] suggest the possibility of an error in that calculation (which used an early version of QRPA<sub>sph</sub> that no longer exists). Our many tests of the current approach make it unlikely that our calculations contain outright errors. The delicacy of  $a_1$ , is noteworthy, however, both because of the complicated spatial  $PT$ -odd density distribution (see fig. 2) and the sometimes marginally stable convergence to axially symmetric solutions, a feature that is particularly pronounced for that coefficient.

How much can we trust the physical approximations underlying our results? The calculations presented here are unquestionably more sophisticated and inclusive than any yet attempted, but it may very well be that still more sophistication is required. The apparent softness of  $^{199}\text{Hg}$  implies that the true ground state is best thought

of as a superposition of many different mean-field states, and a generator-coordinate-based approach [25] may be required to adequately represent the mixing. Though generator-coordinate calculations are no longer rare, they have not, to our knowledge, been attempted yet in odd nuclei. The future of EDM calculations for this kind of nucleus lies in the generalization of codes like HFODD. We will need to move beyond mean-field theory, and ought to expect our current best numbers to be noticeably revised when we do.

This work was supported in part by the U.S. Department of Energy under Contract No. DE-FG02-97ER41019, by the Polish Ministry of Science under Contract No. N N202 328234, and by the Academy of Finland and University of Jyväskylä within the FIDIPRO programme. Shufang Ban would like to acknowledge partial support from DOE grant DE-FG02-87ER40365.

- 
- [1] A. Zee, *Quantum Field Theory in a Nutshell* (Princeton University Press, 2003).
- [2] M. Trodden, *Rev. Mod. Phys.* **71**, 1463 (1999).
- [3] L. I. Schiff, *Phys. Rev.* **132**, 2194 (1963).
- [4] M. Pospelov and A. Ritz, *Annals of Physics* **318**, 119 (2005).
- [5] V. V. Flambaum, I. B. Khriplovich, and O. P. Sushkov, *Nucl. Phys.* **A449**, 750 (1986).
- [6] V. F. Dmitriev and R. A. Sen'kov, *Phys. Atom. Nucl.* **66**, 1940 (2003).
- [7] V. F. Dmitriev, R. A. Sen'kov, and N. Auerbach, *Phys. Rev. C* **71**, 035501 (2005).
- [8] J. de Jesus and J. Engel, *Phys. Rev. C* **72**, 045503 (2005).
- [9] J. Dobaczewski, W. Satuła, B. Carlsson, J. Engel, P. Olbratowski, P. Powalowski, M. Sadziak, N. Schunk, A. Staszczak, M. Stoitsov, et al., *Comp. Phys. Comm.* **180**, 2361 (2009).
- [10] P. Möller, J. R. Nix, W. D. Myers, and W. J. Swiatecki, *At. Dat. Nucl. Dat. Tables* **59**, 185 (1995).
- [11] G. E. Brown, *in Facets of Physics* (Academic Press, New York, 1970).
- [12] J. P. Blaizot and G. Ripka, *Quantum Theory of Finite Systems* (MIT Press, Cambridge, Massachusetts; London, England, 1986), problem 10.14, p. 347.
- [13] N. Schunck, J. Dobaczewski, J. McDonnell, J. Moré, W. Nazarewicz, J. Sarich, and M. V. Stoitsov, *Phys. Rev. C* **81**, 024316 (2010).
- [14] J. Dobaczewski and J. Engel, *Phys. Rev. Lett.* **94**, 232502 (2005).
- [15] J. Engel, M. Bender, J. Dobaczewski, J. H. de Jesus, and P. Olbratowski, *Phys. Rev. C* **68**, 025501 (2003).
- [16] M. Bender, J. Dobaczewski, J. Engel, and W. Nazarewicz, *Phys. Rev. C* **65**, 054322 (2002).
- [17] K. Bennaceur and J. Dobaczewski, *Comput. Phys. Commun.* **168**, 96 (2005).
- [18] J. Terasaki and J. Engel, *Phys. Rev. C* **74**, 044301 (2006).
- [19] J. Bartel, P. Quentin, M. Brack, C. Guet, and H.B. Håkansson, *Nucl. Phys. A* **386**, 79 (1982).
- [20] T. Chupp, private communication.
- [21] E. Chabanat, P. Bonche, P. Haensel, J. Meyer, and R. Schaeffer, *Nucl. Phys. A* **635**, 231 (1998).
- [22] M. Beiner, H. Flocard, N. Van Giai, and P. Quentin, *Nucl. Phys. A* **238**, 29 (1975).
- [23] P.-G. Reinhard, D.J. Dean, W. Nazarewicz, J. Dobaczewski, J.A. Maruhn, and M.R. Strayer, *Phys. Rev. C* **60**, 014316 (1999).
- [24] V. V. Flambaum and J. S. M. Ginges, *Phys. Rev. A* **65**, 032113 (2002).
- [25] P. Ring and P. Schuck, *The Nuclear Many-Body Problem* (Springer-Verlag, New York, Heidelberg, Berlin, 1980).